

Single Crystal X-Ray and Optical Studies on Bis(1,5-diazacyclooctane)-copper(II) Nitrate, a Thermochromic Copper(II) Complex Involving Hydrogen Bonds between the Ligand and the Counter Ion

Naomi HOSHINO,[†] Yutaka FUKUDA,* Kozo SONE, Kiyoaki TANAKA,^{††} and Fumiyuki MARUMO^{††}

Department of Chemistry, Faculty of Science, Ochanomizu University, Otsuka, Bunkyo-ku, Tokyo 112

^{††}Research Laboratory of Engineering Materials, Tokyo Institute of Technology, Nagatsuta, Midori-ku, Yokohama 227

(Received September 27, 1988)

A thermochromic copper(II) complex of 1,5-diazacyclooctane (daco), $[\text{Cu}(\text{daco})_2](\text{NO}_3)_2$, has been subjected to single-crystal X-ray and optical studies. This complex is orange as isolated, but it turns violet discontinuously when heated above 90 °C and returns to orange on cooling. Crystal structure of the low-temperature form has been determined at room temperature; the complex crystallizes in the monoclinic space group $P2_1/n$ with $a=7.9040(7)$, $b=15.694(1)$, $c=7.0886(7)$ Å, $\beta=95.36(1)^\circ$; $V=875.5(1)$ Å³, and $Z=2$. The CuN_4 chelate plane is planar and Cu–N coordination bonds are rather short. The structure has revealed the presence of weak hydrogen bonds bridging imino groups of the ligands with the nitrate ions and forming a macrocycle-like ring system, which results in enhancement of the ligand field strength. Single-crystal visible and infrared spectra for both low- and high-temperature forms have been obtained and compared. A high-energy d–d transition band(s) causing the orange color at room temperature is in contrast to an extremely flattened broad band(s) for the violet form. The IR spectra of the two forms clearly differ in the intensity of ν_{NH} stretching peak, implying that the thermochromic phase transition involves a change in the nature of the hydrogen bonds of the imine ligands. On the basis of these observations and comparison to reported studies on a similarly thermochromic copper(II) complex, a mechanism is suggested involving dynamic fluctuation of the ligand field and geometry due to thermal motion of the anion/ligand hydrogen bond system.

Thermochromism and related chromotropic behaviors of inorganic compounds have been recently reviewed.¹⁾ There exist a number of examples of thermochromic metal complexes and origins of the color changes are quite diverse. A certain class of materials show gradual color change over a wide temperature range, which is called continuous thermochromism.²⁾ Discontinuous thermochromism,²⁾ on the other hand, is a more abrupt or clearly visible color change over a small temperature range and manifests the onset of a first- or second-order phase transition. This latter phenomenon is not only interesting in its own right but also provides information on various factors determining coordination geometries and crystal structures of transition metal complexes.

We have previously reported that a copper(II) complex of 1,5-diazacyclooctane (daco), $[\text{Cu}(\text{daco})_2](\text{NO}_3)_2$, shows reversible thermochromism between orange (at room temperature) and violet (above 90 °C) in solid state.³⁾ It was suggested at the moment that coordination of the nitrate ions to the copper center at elevated temperatures is responsible for the color change. On the other hand, Musker and Hussain have previously studied on bis(daco) complexes of copper(II) and nickel(II) and stated that the boat-chair conformation of the mesocyclic chelate ring would more or less shield the axial site of the central metal atom.^{4,5)} It was revealed later⁶⁾ that the nitrate ion in $[\text{Cu}(\text{daco})_2](\text{NO}_3)_2$ is indeed far from accessible to the copper atom in the axial direction, and is rather interacting laterally with the daco ligands via a pair of

hydrogen bonds. Thus the thermochromic mechanism appears to involve such ligand–anion interaction rather than the metal–anion bonding.

The purpose of this paper is to shed new light on the role of ligand–anion hydrogen bonding interaction in determining the structure, the ligand field strength, and the resulting physical properties of transition metal chelates. The crystal structure and optical spectra of $[\text{Cu}(\text{daco})_2](\text{NO}_3)_2$, obtained for single crystals, are reported herein to show that the daco–nitrate interaction is really a key factor in the thermochromic phase transition of this complex.

Experimental

Materials. Synthesis of daco and $[\text{Cu}(\text{daco})_2](\text{NO}_3)_2$ has been reported elsewhere.^{3,7)} Single crystals of the latter were grown by slow evaporation from an ethanol solution.

Physical Measurements. Single-crystal infrared absorption spectra were measured using an optical system consisting of a JASCO infrared radiation source, a JASCO CT-25C monochromator, an SBRC HgCdTe detector, and a PAR Model 124A lock-in amplifier. Visible absorption spectra were obtained with a similar system comprising a halogen-gas-filled tungsten incandescent lamp, an ISA Jobin Yvon Type HR1000 monochromator, and a Hamamatsu R376 photomultiplier. Polarized spectra were not obtained since the crystal faces were ill-defined.

The thermochromic transition temperature and enthalpy were determined using a Rigaku Thermoflex differential scanning calorimeter at a heating rate of 5 K min^{−1}.

X-Ray Analysis. An orange crystal was shaped into a sphere with a diameter of 0.22 mm on a wet filter paper under a microscope. Weissenberg photographs were taken with $\text{CuK}\alpha$ radiation ($\lambda=1.54184$ Å) and the crystal was found to be monoclinic and has the space group $P2_1/n$.

[†] Present address: Department of Chemistry, Faculty of Science, Hokkaido University, Sapporo 060.

Diffraction data were collected on a Philips automated four-circle diffractometer PW1100 having a maximum 2θ value of 90° with graphite monochromated Mo $K\alpha$ radiation ($\lambda = 0.71073 \text{ \AA}$). Cell constants (Table 1) were obtained from least-squares refinement, on the basis of setting angles of 67 reflections in the range $52^\circ < 2\theta < 74^\circ$, where separation of the $K\alpha$ doublet was clear and only the Mo $K\alpha_1$ reflections were used. A total of 3963 independent reflections were collected, and 2948 reflections ($h = -13$ to 13 , $k = 0$ to 29 , and $l = 0$ to 18) met the condition $I > 3\sigma(I)$ to be used for subsequent analysis. Three standard reflections ($hkl = 400, 080$, and 004) were measured every 50 reflections and no significant variation was detected. Each reflection was measured up to 8 times until the total peak count exceeded 40000. Lorentz-polarization correction and absorption correction (factors ranging between 1.245 and 1.250) were applied to the data.

The structure was solved by the direct method with MULTAN78,⁸⁾ which yielded positions of all the nonhydrogen atoms. The structure was refined by the full-matrix least-squares method with the program LINKT80,⁹⁾ which minimizes the function $\sum(|F_o| - |F_c|)^2$; unit weight was assigned

to each reflection. Hydrogen atoms were located on difference Fourier maps and their positions were refined with isotropic temperature factors, while anisotropic temperature factors were refined for nonhydrogen atoms. Anisotropic Type I extinction parameters were also refined.¹⁰⁾ The final values for R and R_w were 0.0311 and 0.0315, respectively. The maximum shift in the final cycle of the least-squares refinement was 0.15 for the isotropic temperature factor of H(12). The final difference Fourier map was featureless. Atomic scattering factors and dispersion terms were taken from the literature.¹¹⁾ Tables of temperature factors and structure factors are deposited as Document No.8878 at the Office of the Editor of Bull. Chem Soc. Jpn.

Results and Discussion

Crystal Structure of $[\text{Cu}(\text{daco})_2](\text{NO}_3)_2$ at Room Temperature. This is the first example of bis(daco) complex of copper(II) for which the crystal structure has been solved. Figure 1 shows the structure, determined at room temperature, together with the numbering scheme. A stereoview showing crystal packing is given in Fig. 2. Table 2 lists atomic positional parameters, and selected interatomic distances and bond lengths and angles are summarized in Table 3.

The structure is centrosymmetric with the center of symmetry on the site of Cu and the CuN_4 chelate plane is planar. But it is not precisely square since two Cu-N coordination bonds of a daco ligand differ in length significantly ($1.997(1) \text{ \AA}$ for Cu-N(1) and $2.034(1) \text{ \AA}$ for Cu-N(2)). These bond lengths, particularly of the former, are rather short for a Cu(II)-N(secondary amine) bond.¹²⁾ These facts agree with an enhanced ligand field strength suggested by the orange color which is rarely encountered among copper(II) com-

Table 1. Crystallographic Data for $[\text{Cu}(\text{daco})_2](\text{NO}_3)_2$

Formula	$\text{CuC}_{12}\text{H}_{28}\text{N}_6\text{O}_6$
Fw	415.94
Space group	$P2_1/n$
$a/\text{\AA}$	7.9040(7)
$b/\text{\AA}$	15.694(1)
$c/\text{\AA}$	7.0886(7)
β/deg	95.36(1)
$V/\text{\AA}^3$	875.5(1)
Z	2
$d_{\text{calcd}}/\text{g cm}^{-3}$	0.7889
$F(000)$	438
$\mu/\text{cm}^{-1} (\text{Mo } K\alpha)$	13.42

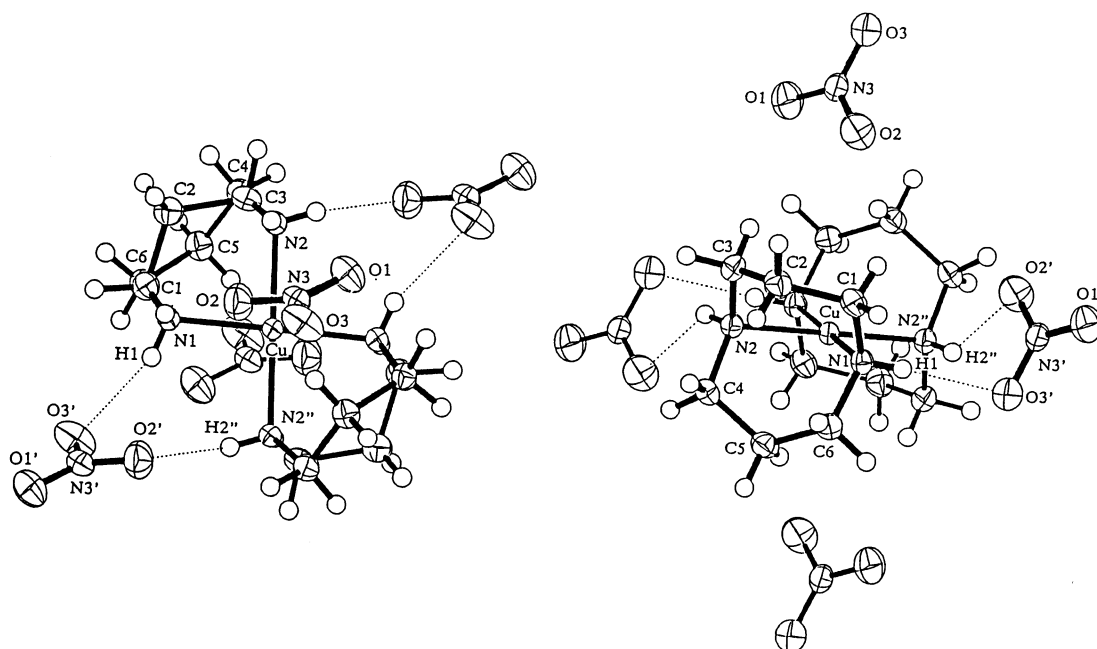
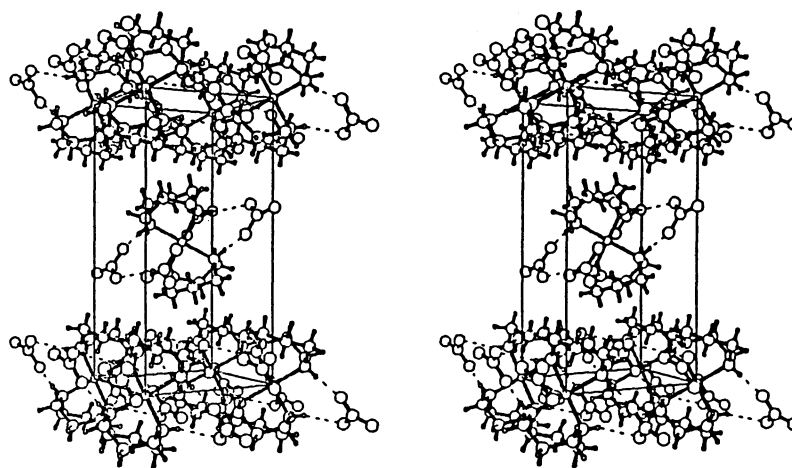


Fig. 1. Perspective drawings of $[\text{Cu}(\text{daco})_2](\text{NO}_3)_2$ with thermal ellipsoids scaled to 40% probability and atomic numbering scheme. The atoms labeled by ' and '' are generated by symmetry operations, $(-x, -y, 1-z)$ and $(-x, -y, -z)$, respectively.

Fig. 2. Stereoview of crystal packing for $[\text{Cu}(\text{daco})_2](\text{NO}_3)_2$.Table 2. Fractional Atomic Coordinates and Equivalent Thermal Parameters, $B_{\text{eq}}(\text{\AA}^2)$, for $[\text{Cu}(\text{daco})_2](\text{NO}_3)_2$

$$B_{\text{eq}} = \frac{4}{3} \sum_i \sum_j B_{ij} a_i a_j$$

Atom ^{a)}	<i>x</i>	<i>y</i>	<i>z</i>	$B_{\text{eq}}/\text{\AA}^2$
Cu	0.0	0.0	0.0	1.791(5)
N(1)	0.0663(2)	-0.11025(7)	0.1266(2)	2.20(3)
N(2)	-0.2147(2)	-0.06144(7)	-0.1058(2)	2.15(3)
N(3)	-0.3582(2)	0.09057(9)	0.4851(2)	2.88(3)
O(1)	-0.4166(2)	0.1162(1)	0.3279(2)	5.03(7)
O(2)	-0.2716(2)	0.02510(9)	0.5014(2)	4.71(7)
O(3)	-0.3820(2)	0.1316(1)	0.6316(2)	5.37(9)
C(1)	-0.0543(2)	-0.1298(1)	0.2699(2)	2.87(4)
C(2)	-0.2329(2)	-0.1499(1)	0.1852(3)	3.12(4)
C(3)	-0.3161(2)	-0.0820(1)	0.0555(3)	2.87(4)
C(4)	-0.1794(2)	-0.1371(1)	-0.2244(2)	2.60(8)
C(5)	0.0081(3)	-0.1587(1)	-0.2091(3)	2.97(4)
C(6)	0.0874(2)	-0.1806(1)	-0.0118(3)	2.74(4)
H(1)	0.156(3)	-0.105(1)	0.185(3)	3.12(5)
H(2)	-0.271(3)	-0.028(1)	-0.171(3)	3.3(1)
H(3)	-0.009(3)	-0.179(2)	0.347(3)	3.78(6)
H(4)	-0.054(3)	-0.082(2)	0.348(3)	3.80(6)
H(5)	-0.235(3)	-0.202(1)	0.121(3)	3.13(5)
H(6)	-0.301(3)	-0.158(2)	0.288(3)	4.05(7)
H(7)	-0.332(3)	-0.032(2)	0.122(3)	3.59(6)
H(8)	-0.429(3)	-0.099(1)	0.008(3)	3.75(6)
H(9)	-0.213(3)	-0.123(2)	-0.356(4)	4.17(7)
H(10)	-0.244(3)	-0.184(1)	-0.186(3)	3.31(5)
H(11)	0.071(3)	-0.113(2)	-0.259(4)	4.29(8)
H(12)	0.021(3)	-0.208(2)	-0.292(4)	4.71(8)
H(13)	0.041(3)	-0.231(1)	0.035(3)	3.27(5)
H(14)	0.211(3)	-0.189(1)	-0.010(3)	3.52(6)

a) Hydrogen atoms H(3) through H(14) are numbered in the order of attached carbon atoms C(1) through C(6).

plexes. An important feature to note is that each $[\text{Cu}(\text{daco})_2]^{2+}$ unit carries two NO_3^- ions which are hydrogen bonded to the amino nitrogens. These hydrogen bonds form a macrocycle-like ring system including a pair of $\text{N}(1)-\text{H}(1)-[\text{O}(3)'\text{-N}(3)'\text{-O}(2)']\text{-H}(2)''\text{-N}(2)''$ bridges (dotted lines in Fig. 1). But these bonds are relatively weak; the interatomic distances

2.912(2) \AA ($\text{N}(1)\cdots\text{O}(3)'$) and 3.093(2) \AA ($\text{N}(2)''\cdots\text{O}(2)'$) are both in the range of weak hydrogen bond distances.¹³⁾ The positions of the hydrogen atoms which have been determined clearly demonstrate that these hydrogen bonds are not equivalent; the plane of NO_3^- is tilted by 68.2° relative to the CuN_4 chelate plane within which the $\text{O}(3)'$ atom and both of the hydrogen atoms H(1) and H(2)'' reside (Fig. 1, right), and so the $\text{N}(1)-\text{H}(1)-\text{O}(3)'$ hydrogen bond is rather straight ($161(2)^\circ$) while the $\text{N}(2)''\text{-H}(2)''\text{-O}(2)'$ bond is bent ($136(2)^\circ$). As a consequence of this unsymmetrical interaction of the anion to the ligand, not only the symmetry of the NO_3^- ion deviates from D_{3h} but also the two coordination bond lengths are significantly different as mentioned above; more linear and shorter hydrogen bond $\text{N}(1)-\text{H}(1)-\text{O}(3)'$ makes the related coordination bond $\text{Cu}-\text{N}(1)$ shorter than the other.

Although the axial nitrate ions in Fig. 2 appear to have a close contact to the metal centers to form one-dimensional arrays of the chelate cations, such axial coordination does not exist, since even the shortest axial distance is 4.338(2) \AA for $\text{Cu}\cdots\text{O}(2)$. This situation is well illustrated in the side view of the complex shown on the right in Fig. 1. The axial coordination appears to be precluded by chair and boat conformations of the chelate rings involving C(1)-C(2)-C(3) and C(4)-C(5)-C(6), respectively.

It is interesting to compare the structure with those of analogous species. Boeyens and Fox determined the structure of $[\text{Ni}(\text{daco})_2](\text{B}(\text{C}_6\text{H}_5)_4)_2 \cdot 2\text{DMSO}$ and stated that the two solvent molecules, located aside the chelate plane, are interacting with the diamine nitrogen atoms through hydrogen bonding.¹⁴⁾ In addition, redetermination of the crystal structure of $[\text{Ni}(\text{daco})_2](\text{ClO}_4)_2 \cdot 2\text{H}_2\text{O}$ by Boeyens et al. revealed that the water molecules also act as bridges between neighboring chelate cations through a set of $\text{O}-\text{H}-\text{N}$ hydrogen bonds.¹⁵⁾ Thus the hydrogen bonding in crystals of daco complexes seems to be not uncom-

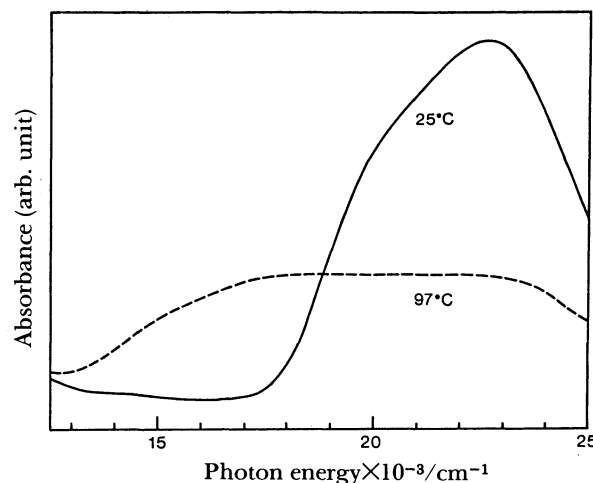
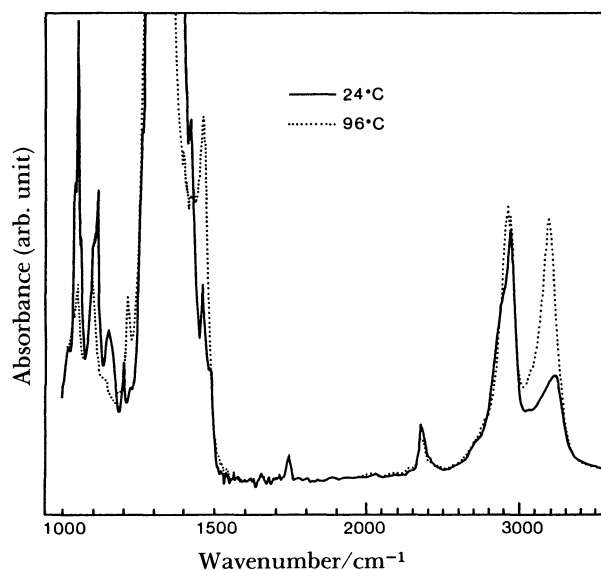
Table 3. Selected Interatomic and Bond Distances (Å) and Bond Angles (deg) in $[\text{Cu}(\text{daco})_2](\text{NO}_3)_2$

Cu-N(1)	1.997(1)	N(3)'H...(2)''	3.10(2)
Cu-N(2)	2.034(1)	O(2)'...H(2)''	2.47(2)
Cu...N(3)	4.866(2)	O(3)'...H(1)	2.15(2)
Cu...O(1)	4.583(2)	C(1)-C(2)	1.515(3)
Cu...O(2)	4.338(2)	C(1)-C(6)	2.508(3)
Cu...N(3)'	4.629(1)	C(1)-H(3)	0.99(2)
Cu...O(2)'	3.980(2)	C(1)-H(4)	0.93(2)
Cu...O(3)'	4.328(2)	C(2)-C(3)	1.517(3)
N(1)-C(1)	1.488(2)	C(2)-H(5)	0.94(2)
N(1)-C(6)	1.496(2)	C(2)-H(6)	0.95(3)
N(1)-H(1)	0.79(2)	C(3)-H(7)	0.93(2)
N(1)...O(3)'	2.912(2)	C(3)-H(8)	0.96(2)
N(2)-C(3)	1.491(2)	C(4)-C(5)	1.514(3)
N(2)-C(4)	1.496(2)	C(4)-H(9)	0.97(2)
N(2)-H(2)	0.80(2)	C(4)-H(10)	0.95(2)
N(2)'...O(2)'	3.093(2)	C(5)-C(6)	1.517(2)
N(3)-O(1)	1.233(2)	C(5)-H(11)	0.95(3)
N(3)-O(2)	1.234(2)	C(5)-H(12)	0.99(3)
N(3)-O(3)	1.251(2)	C(6)-H(13)	0.95(2)
N(3)'...H(1)	2.72(2)	C(6)-H(14)	0.99(2)
N(1)-Cu-N(2)	85.98(5)	C(3)-C(2)-H(6)	108(2)
Cu-N(1)-C(1)	109.1(1)	H(5)-C(2)-H(6)	106(2)
Cu-N(1)-C(6)	112.67(9)	N(2)-C(3)-C(2)	112.6(1)
Cu-N(1)-H(1)	109(2)	N(2)-C(3)-H(7)	108(1)
C(1)-N(1)-C(6)	114.4(1)	N(2)-C(3)-H(8)	110(1)
C(1)-N(1)-H(1)	106(2)	C(2)-C(3)-H(7)	111(1)
C(6)-N(1)-H(1)	106(2)	C(2)-C(3)-H(8)	111(1)
Cu-N(2)-C(3)	108.0(1)	H(7)-C(3)-H(8)	104(2)
Cu-N(2)-C(4)	112.98(9)	N(2)-C(4)-C(5)	111.8(1)
Cu-N(2)-H(2)	108(2)	N(2)-C(4)-H(9)	108(1)
C(3)-N(2)-C(4)	113.6(1)	N(2)-C(4)-H(10)	109(1)
C(3)-N(2)-H(2)	106(2)	C(5)-C(4)-H(9)	107(1)
C(4)-N(2)-H(2)	108(2)	C(5)-C(4)-H(10)	111(1)
O(1)-N(3)-O(2)	120.9(2)	H(9)-C(4)-H(10)	110(2)
O(1)-N(3)-O(3)	120.6(2)	C(4)-C(5)-C(6)	115.7(2)
O(2)-N(3)-O(3)	118.4(2)	C(4)-C(5)-H(11)	110(2)
N(3)'-O(2)'...H(2)''	108.9(6)	C(4)-C(5)-H(12)	107(2)
N(3)'-O(3)'...H(1)	102.7(6)	C(6)-C(5)-H(11)	109(2)
N(1)-C(1)-C(2)	113.9(1)	C(6)-C(5)-H(12)	108(2)
N(1)-C(1)-H(3)	108(1)	H(11)-C(5)-H(12)	106(2)
N(1)-C(1)-H(4)	106(2)	N(1)-C(6)-C(5)	112.1(1)
C(2)-C(1)-H(3)	110(1)	N(1)-C(6)-H(13)	109(1)
C(2)-C(1)-H(4)	111(2)	N(1)-C(6)-H(14)	105(1)
H(3)-C(1)-H(4)	108(2)	C(5)-C(6)-H(13)	112(1)
C(1)-C(2)-C(3)	115.4(2)	C(5)-C(6)-H(14)	111(1)
C(1)-C(2)-H(5)	110(1)	H(13)-C(6)-H(14)	107(2)
C(1)-C(2)-H(6)	107(2)	N(1)-H(1)...O(3)'	161(2)
C(3)-C(2)-H(5)	110(1)	N(2)''-H(2)''...O(2)'	136(2)

mon; as will be discussed below, we believe that the subtleness of this interaction is closely related to the thermochromic phase transition in the case of $[\text{Cu}(\text{daco})_2](\text{NO}_3)_2$.

It would be desirable to have crystal structure of the high temperature form as well, but it has not been possible to date due to crystal disintegration on prolonged heating.

Optical and EPR Spectral Changes Associated with Thermochromism of $[\text{Cu}(\text{daco})_2](\text{NO}_3)_2$. The reversible thermochromism of $[\text{Cu}(\text{daco})_2](\text{NO}_3)_2$ can be visually observed as a distinct color change of a powdered

Fig. 3. Single-crystal visible spectral change associated with thermochromism of $[\text{Cu}(\text{daco})_2](\text{NO}_3)_2$.Fig. 4. Single-crystal infrared spectral change upon thermochromic transition of $[\text{Cu}(\text{daco})_2](\text{NO}_3)_2$.

sample between orange and violet, as mentioned above. Powder reflectance spectral changes corresponding to this behavior were previously reported.³⁾ Single crystals have been used in this work in order to obtain absorption data which can be directly compared with each other. The results are shown in Figs. 3 and 4 for visible and infrared regions, respectively.

The visible absorption spectrum of $[\text{Cu}(\text{daco})_2](\text{NO}_3)_2$ recorded at 25°C exhibits a broad band which peaks at $22.7 \times 10^3 \text{ cm}^{-1}$ and shows a shoulder at $20.0 \times 10^3 \text{ cm}^{-1}$. As the crystal is heated with the peak intensity monitored, this band slightly diminishes at first and then suddenly drops to about one third of the original intensity at around 90°C. The spectrum recorded at 97°C indicates also that the absorption band is now widely spread (Fig. 3).

Royer et al. have investigated single-crystal polar-

ized spectra of $[\text{Cu}(\text{daco})_2](\text{ClO}_4)_2 \cdot 2\text{H}_2\text{O}$, and deduced with some assumptions that the d-orbital energy order is $b_{1g} \gg b_{2g} > e_g > a_{1g}$ under D_{4h} symmetry.¹⁶⁾ According to their Gaussian resolution of the spectra, the visible band of this perchlorate salt is composed of three components; ${}^2B_{1g} \rightarrow {}^2B_{2g}$ at $18.2 \times 10^3 \text{ cm}^{-1}$, ${}^2B_{1g} \rightarrow {}^2E_g$ at $20.8 \times 10^3 \text{ cm}^{-1}$, and ${}^2B_{1g} \rightarrow {}^2A_{1g}$ at $23.1 \times 10^3 \text{ cm}^{-1}$. Polarization experiments were not performed in this study, but it seems that the Gaussian fitting would become more arbitrary; it requires four components, since at least the crystal structure at room temperature has shown that the effective ligand field symmetry in $[\text{Cu}(\text{daco})_2](\text{NO}_3)_2$ is no higher than D_{2h} . However, we can still apply the fundamental scheme obtained for the perchlorate analogue that strong σ interaction of the daco ligand raises the energy of $d_{x^2-y^2}$ orbital up high, while the rest of d-orbitals are lying low and relatively close to each other. It is notable in Fig. 3 that, regardless of possible spectral resolution, even the lowest energy transition component with significant intensity should appear at the energy no lower than $\text{ca. } 20 \times 10^3 \text{ cm}^{-1}$ for the room temperature spectrum. This suggests that the σ -interaction of the ligand is stronger in the nitrate salt than in the perchlorate salt. This could well be due to the ligand-nitrate hydrogen bonds enhancing rigidity of the planar coordination geometry and also basicity of the donor nitrogen atoms.

On the other hand, the spectrum recorded at 97°C indicates at least that some of the d-d transition components have shifted towards lower energy. This can be interpreted as a result of weakening of the ligand field and/or a change in its symmetry; not only is the energy of $d_{x^2-y^2}$ orbital lowered but also the relative spacings among the rest of d-orbitals must have changed, as suggested by the spectral breadth.

A piece of evidence for correlation of the hydrogen bonding to the thermochromic phase transition was obtained from infrared measurements. Comparison of the IR spectra of $[\text{Cu}(\text{daco})_2](\text{NO}_3)_2$ at 24°C and at 96°C , shown in Fig. 4, reveals that most drastic change occurs in the absorption peaks assignable to ν_{NH} stretching mode, which should be sensitive to the nature of the hydrogen bond. Intensification of the peak at 3200 cm^{-1} upon heating can be viewed as release of the intensity of this mode which has been suppressed in the low-temperature phase. However, the shift in its energy is minimal, suggesting that the "average" hydrogen bond strength is not much changed in the two phases. Another noticeable intensification upon heating occurs to a peak at 1460 cm^{-1} , which may be assigned to δ_{NH} deformation. Stretching absorption of the NO_3^- ion is too intense to assess a change with temperature on this side of the hydrogen bond. It is noted, however, that a small peak at 1747 cm^{-1} , which can be a combination band of NO_3^- modes, shows no detectable change in shape.

If this complex nitrate is ground together with KBr,

resulting powder mixture is colored violet and the IR spectrum of this KBr disk is identical to that of $[\text{Cu}(\text{daco})_2]\text{Br}_2 \cdot \text{H}_2\text{O}$,¹⁷⁾ with a characteristic sharp peak at 1649 cm^{-1} , indicating that NO_3^- can be easily relaxed by Br^- . It is likely that one of the bromide ions is coordinated to copper in the violet bromide salt,¹⁷⁾ and this inclines one to assume a similar anion coordination in the high-temperature violet form of nitrate salt which is apparently similar in color. However, an EPR evidence has shown that the two violet species are different in terms of the ligand field strength and symmetry. Figure 5 compares the powder EPR spectra of low- and high-temperature forms of $[\text{Cu}(\text{daco})_2](\text{NO}_3)_2$ and $[\text{Cu}(\text{daco})_2]\text{Br}_2 \cdot \text{H}_2\text{O}$. The g -values for the former are $g_{\parallel}=2.142$ and $g_{\perp}=2.033$, which are practically constant from room temperature up to the transition temperature (orange form, Fig. 5a) and change to $g_{\parallel}=2.122$ and $g_{\perp}=2.046$ (violet form, Fig. 5b). Those for the bromide salt, on the other hand, are $g_{\parallel}=2.169$ and $g_{\perp}=2.031$ (Fig. 5c). Thus the thermochromic transition of the nitrate salt is associated with decreases in the g_{\parallel} value and in the anisotropy of the g -values at the elevated temperatures. This behavior is opposite to what would be expected if the anion coordinates axially to the metal center upon heating.¹⁸⁾ What then would be the cause for the color change of the nitrate salt?

On the Mechanism of Thermochromism. The thermochromic phase transition of $[\text{Cu}(\text{daco})_2](\text{NO}_3)_2$ occurs endothermically at 85.5°C (at a heating rate of 5 K min^{-1} , $\Delta H=7.61 \text{ kJ mol}^{-1}$). Solid-state thermochromism has been observed among other metal complexes of daco ligand,^{4,5)} but in these cases (e.g., $\text{Co}(\text{daco})_2\text{I}_2 \cdot \text{EtOH}$ ⁵⁾ and $\text{Cu}(\text{daco})_2\text{X}_2 \cdot \text{H}_2\text{O}$ ($\text{X}=\text{Br}, \text{Cl}$)¹⁷⁾) the observed color changes involve dehydration

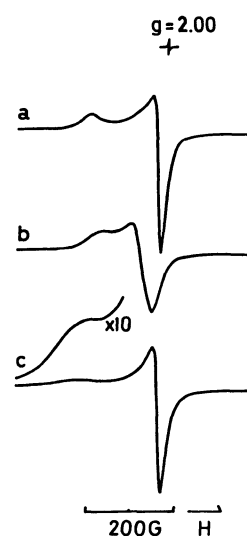


Fig. 5. Powder EPR spectra for (a) orange form and (b) violet form of $[\text{Cu}(\text{daco})_2](\text{NO}_3)_2$, and (c) $\text{Cu}(\text{daco})_2\text{Br}_2 \cdot \text{H}_2\text{O}$ (violet). Spectra were recorded at the apparent cavity temperatures of 99.7°C for (a) and (c) and of 120°C for (b).

or desolvation at relatively high temperatures. On the other hand, there exists a broader class of materials containing *N,N*-diethylethylenediamine (deen) which exhibit thermochromic phase transition, and among them $[\text{Cu}(\text{deen})_2](\text{ClO}_4)_2$ has been most extensively investigated. Bloomquist and Willett has reviewed²⁾ the work on this compound including crystal structure determination for both low- and high-temperature forms.¹²⁾ A short summary will be given below to facilitate comparison between $[\text{Cu}(\text{daco})_2](\text{NO}_3)_2$ and $[\text{Cu}(\text{deen})_2](\text{ClO}_4)_2$ that follows.

This compound is red at room temperature, and changes to deep blue-purple at $T_{\text{th}}=43^\circ\text{C}$ ($\Delta H=8.91\text{ kJ mol}^{-1}$) returning to red upon cooling. Mechanistic interpretation for this behavior based on EPR and IR spectroscopies ascribed it to axial interaction of the perchlorate ion, since the evidences suggested an increase in the in-plane ligand field at lower temperatures. However, X-ray crystallographic analyses revealed that the perchlorate ions are isolated from the Cu(II) coordination sphere in both phases; the closest $\text{Cu}\cdots\text{O}$ distance is $3.65(1)\text{ \AA}$ and $4.16(2)\text{ \AA}$ in the low- and high-temperature form, respectively. It was thus concluded that the thermochromic change in $[\text{Cu}(\text{deen})_2](\text{ClO}_4)_2$ must be due to a sudden change of the in-plane ligand field strength caused by conformational changes in the $\text{Cu}(\text{en})_2$ ring system.¹²⁾ Bloomquist and Willett noticed that each perchlorate ion is involved in two $\text{N}-\text{H}\cdots\text{O}$ hydrogen bonds with chelate cations (here also) at room temperature and stated further that, "as the temperature is raised, a point is reached at which the thermal motion energy sufficiently weakens the hydrogen bonding network to allow the two Cu-diamine ring systems to begin rapid conformational interconversion." A puzzling part of the results of the above crystallographic study is that the Cu-N bond lengths hardly differ between the two phases, raising a question as to why the change in the in-plane ligand field strength is not reflected in these parameters. This, however, was explained in terms of the ligand disorder, dynamic in nature, preventing optimal Cu-N overlap in the high-temperature blue modification.

Returning to the present case of $[\text{Cu}(\text{daco})_2](\text{NO}_3)_2$, it is not possible to fully delineate the thermochromic mechanism at the present stage without a complete set of structural evidences. However, the data available at present seem to indicate that this picture of "dynamic" disorder will apply to the case of $[\text{Cu}(\text{daco})_2](\text{NO}_3)_2$ just as well or even better. It should be emphasized that the visible absorption spectral change accompanying the phase transition of $[\text{Cu}(\text{daco})_2](\text{NO}_3)_2$ is not a simple shift of a certain d-d transition. It has been conveniently and perhaps reasonably assumed for $[\text{Cu}(\text{deen})_2](\text{ClO}_4)_2$ that the visible absorption can be ascribed to the $d_{xz}, d_{yz}\rightarrow d_{x^2-y^2}$ transition with the effective ligand field symmetry D_{4h} and that this band shifts up and down according to the

variation in the in-plane ligand field. However, the discontinuous absorption spectral change with temperature for $[\text{Cu}(\text{daco})_2](\text{NO}_3)_2$ appears to involve a rather drastic change in d-orbital energy scheme. The very broad and flat shape of the visible absorption band for the high-temperature form implies that mixing among the d-orbitals has become extensive. The infrared spectral change also suggests that the hydrogen bond strength in a static sense does not change on heating. Thus a simple picture of weakening of the in-plane ligand field due to thermal motion of the ligand and/or to weakening of the ligand/anion hydrogen bonds is not sufficient to explain the thermochromic transition in $[\text{Cu}(\text{daco})_2](\text{NO}_3)_2$.

Therefore, we would like to point out the possibility that the anions play an active role as a source of disorder in the thermochromic transition of this complex, as suggested in the case of $[\text{Cu}(\text{deen})_2](\text{ClO}_4)_2$.²⁾ It can be easily imagined that the thermal motion of the anions would create dynamical fluctuation in the hydrogen bond strength, with protons shifting back and forth, and in the electron density on the ligand nitrogen atoms. It is recalled that the perchlorate group in $[\text{Cu}(\text{deen})_2](\text{ClO}_4)_2$ (blue) showed anisotropic temperature factors no smaller than those of the ligand.¹²⁾ In the case of $[\text{Cu}(\text{daco})_2](\text{NO}_3)_2$, extensive librational movements of the nitrate ions within the macrocycle-like chelate ring would also induce some distortion in the planar coordination geometry.

Thus the thermochromism of $[\text{Cu}(\text{daco})_2](\text{NO}_3)_2$ seems to have much part of its origin in the anion/ligand hydrogen bond system. Little attention has been paid to the ability of the anions in metal complexes to form hydrogen bonds to the ligands, and to influence the mode and strength of their coordination, while a number of cationic chelates with ligands which are bulky enough to preclude coordination of the anions to the metal center are known. It certainly deserves more studies to exploit this type of interaction, in order to generate novel physical properties of coordination compounds in solid state.

This work was partially supported by a Grant-in-Aid for Scientific Research from Ministry of Education, Science and Culture (No. 59430009). The authors thank the Computer Center, Institute for Molecular Science (IMS), Okazaki National Institutes for the use of HITAC M-680H. We also thank Dr. Takenaka and Prof. Yoshio Sasada of Tokyo Institute of Technology for the drawing program DCMS82 used in the preparation of Figs. 1 and 2. Assistance of Prof. Tadaoki Mitani of IMS in the single crystal optical measurements is greatly appreciated.

References

- 1) K. Sone and Y. Fukuda, "Inorganic Thermochrom-

ism," Springer, Heidelberg (1987).

2) D. R. Bloomquist and R. D. Willett, *Coord. Chem. Rev.*, **47**, 125 (1982).

3) S. Yamaki, Y. Fukuda, and K. Sone, *Chem. Lett.*, **1982**, 269.

4) W. K. Musker and M. S. Hussain, *Inorg. Chem.*, **5**, 1416 (1966).

5) W. K. Musker and M. S. Hussain, *Inorg. Chem.*, **8**, 528 (1969).

6) K. Tanaka, F. Marumo, Y. Fukuda, and K. Sone, The 31st Conference on Coordination Chemistry, Sendai, 1981, Abstr., No. 3C09.

7) E. L. Buhle, A. M. Moore, and F. Y. Wiseloge, *J. Am. Chem. Soc.*, **65**, 29 (1943).

8) P. Main, S. E. Hull, L. Lessinger, G. Germain, J. -P. Declercq, and M. M. Woolfson, MULTAN78, Univ. of York, England, and Univ. of Louvain, Belgium (1978).

9) K. Tanaka and F. Marumo, *Acta Crystallogr., Sect. A*, **39**, 631 (1983).

10) P. J. Becker and P. Coppens, *Acta Crystallogr., Sect. A*, **30**, 129 (1974); **30**, 148 (1974); **31**, 417 (1975);

11) Atomic scattering factors for nonhydrogen atoms were taken from "International Tables for X-Ray Crystallography," ed by J. A. Ibers and W. C. Hamilton, Kynoch Press, Birmingham (1974), Vol. IV and those for hydrogen atoms from R. F. Stewart, E. R. Davidson, and W. T. Simpson, *J. Chem. Phys.*, **42**, 3185 (1965).

12) I. Grenthe, P. Paoletti, M. Sandstroem, and S. Glikberg, *Inorg. Chem.*, **18**, 2687 (1979).

13) G. H. Stout and L. H. Jensen, "X-Ray Structure Determination: A Practical Guide," MacMillan, New York (1968).

14) J. C. A. Boeyens and C. C. Fox, *S. Afr. J. Chem.*, **37**, 1 (1984).

15) J. C. A. Boeyens, C. C. Fox, and R. D. Hancock, *Inorg. Chim. Acta*, **87**, 1 (1984).

16) D. J. Royer, V. H. Schievelbein, A. R. Kalyanaraman, and J. A. Bertrand, *Inorg. Chim. Acta*, **6**, 307 (1972).

17) N. Hoshino, J. Kawashima, S. Yamaki, Y. Fukuda, and K. Sone, unpublished results.

18) H. Yokoi, M. Sai, and T. Isobe, *Bull. Chem. Soc. Jpn.*, **42**, 2232 (1969).
